



Radiation belt electron precipitation by man-made VLF transmissions

R. Gamble, C.J. Rodger, M.A. Clilverd, Jean-André Sauvaud, N.R. Thomson, S.A. Stewart, R.J. McCormick, Michel Parrot, Jean-Jacques Berthelier

► To cite this version:

R. Gamble, C.J. Rodger, M.A. Clilverd, Jean-André Sauvaud, N.R. Thomson, et al.. Radiation belt electron precipitation by man-made VLF transmissions. *Journal of Geophysical Research Space Physics*, 2008, 113 (A10), pp.A10211. 10.1029/2008JA013369 . hal-00332784

HAL Id: hal-00332784

<https://hal.science/hal-00332784>

Submitted on 8 Feb 2016

HAL is a multi-disciplinary open access archive for the deposit and dissemination of scientific research documents, whether they are published or not. The documents may come from teaching and research institutions in France or abroad, or from public or private research centers.

L'archive ouverte pluridisciplinaire **HAL**, est destinée au dépôt et à la diffusion de documents scientifiques de niveau recherche, publiés ou non, émanant des établissements d'enseignement et de recherche français ou étrangers, des laboratoires publics ou privés.

Radiation belt electron precipitation by man-made VLF transmissions

Rory J. Gamble,¹ Craig J. Rodger,¹ Mark A. Clilverd,² Jean-André Sauvaud,³
Neil R. Thomson,¹ S. L. Stewart,¹ Robert J. McCormick,¹ Michel Parrot,⁴
and Jean-Jacques Berthelier⁵

Received 4 May 2008; revised 14 July 2008; accepted 29 July 2008; published 21 October 2008.

[1] Enhancements of drift-loss cone fluxes in the inner radiation belt have been observed to coincide with the geographic location of the powerful VLF transmitter NWC. In this paper we expand upon the earlier study to examine the occurrence frequency of drift-loss cone enhancements observed above transmitters and the intensity of the flux enhancements and to demonstrate the linkage to transmitter operation. Our study has confirmed the strong dependence that these enhancements have upon nighttime ionospheric conditions. No enhancements were observed during daytime periods, consistent with the increased ionospheric absorption. We have also confirmed the persistent occurrence of the wisp features east of the NWC transmitter. The enhancements are initially observed within a few degrees west of NWC and are present in 95% of the nighttime orbital data east of the transmitter for time periods when the transmitter is broadcasting. No enhancements are observed when NWC is not broadcasting. This provides conclusive evidence of the linkage between these drift-loss cone electron flux enhancements and transmissions from NWC. When contrasted with periods when NWC is nonoperational, there are typically ~ 430 times more 100–260 keV resonant electrons present in the drift-loss cone across $L = 1.67$ – 1.9 owing to NWC transmissions. There are almost no wisp-like enhancements produced by the transmitter NPM, despite its low-latitude location and relatively high output power. The lack of any wisp enhancement for $L < 1.6$ suggests that nonducted propagation is an inefficient mechanism for scattering electrons, which explains the lower cutoff in L of the NWC-generated wisps and the lack of NPM-generated wisps.

Citation: Gamble, R. J., C. J. Rodger, M. A. Clilverd, J.-A. Sauvaud, N. R. Thomson, S. L. Stewart, R. J. McCormick, M. Parrot, and J.-J. Berthelier (2008), Radiation belt electron precipitation by man-made VLF transmissions, *J. Geophys. Res.*, **113**, A10211, doi:10.1029/2008JA013369.

1. Introduction

[2] The behavior of high-energy electrons trapped in the Earth's Van Allen radiation belts has been extensively studied, through both experimental and theoretical techniques. During quiet times, energetic radiation belt electrons are distributed into two belts divided by the “electron slot” at $L \sim 2.5$, near which there is relatively low energetic electron flux. In the more than four decades since the discovery of the belts [Van Allen *et al.*, 1958; Van Allen, 1997], it has proven difficult to confirm the principal source

and loss mechanisms that control radiation belt particles [Walt, 1996]. It is well known that large-scale injections of energetic particles into the outer radiation belts are associated with geomagnetic storms which can result in a 10^5 -fold increase in the total trapped electron population [Li and Temerin, 2001]. In some cases the relativistic electron fluxes present in the radiation belts may increase by more than 2 orders of magnitude [Reeves *et al.*, 2003]. In most cases, however, these injections do not penetrate into the inner radiation belt. Only in the biggest storms, for example November 2003, does the slot region fill and the inner belt gain a new population of energetic electrons [e.g., Baker *et al.*, 2004].

[3] Even before the discovery of the radiation belts, high-altitude nuclear explosions (HANEs) were studied as a source for injecting electrons in the geomagnetic field. This was confirmed by the satellite Explorer IV in 1958, when three nuclear explosions conducted under Operation Argus took place in the South Atlantic, producing belts of trapped electrons from the β decay of the fission fragments. The trapped particles remained stable for several weeks near

¹Department of Physics, University of Otago, Dunedin, New Zealand.

²Physical Sciences Division, British Antarctic Survey, NERC, Cambridge, UK.

³Centre d'Étude Spatiale des Rayonnements, Toulouse, France.

⁴Laboratoire de Physique et Chimie de l'Environnement, Orleans, France.

⁵Centre d'Études des Environnements Terrestre et Planétaires, Saint Maur des Fosses, France.

$L = 2$, and did not drift in L or broaden appreciably [Hess, 1968]. Following on from Operation Argus, both the U.S. and USSR conducted a small number of HANEs, all of which produced artificial belts of trapped energetic electrons in the Earth's radiation belts. One of the most studied was the U.S. "Starfish Prime" HANE, a 1.4 Megaton detonation occurring at 400 km above Johnston Island in the central Pacific Ocean on 9 July 1962. Again an artificial belt of trapped energetic electrons was injected, although over a wide range of L shells from about $L = 1.25$ out to perhaps $L = 3$ [Hess, 1968]. The detonation also caused artificial aurora observed as far away as New Zealand, and an electromagnetic pulse which shut down communications and electrical supply in Hawaii, 1300 km away [Dupont, 2004].

[4] The artificial belts produced by this Starfish Prime HANE allowed some understanding of the loss of energetic electrons from the radiation belts, as demonstrated by the comparison of calculated decay rates with the observed loss of injected electrons [Walt, 1994, Figure 7.3]. Collisions with atmospheric constituents are the dominant loss process for energetic electrons (>100 keV) only in the innermost parts of the radiation belts ($L < 1.3$) [Walt, 1996]. For higher L shells, radiation belt particle lifetimes are typically many orders of magnitude shorter than those predicted owing to atmospheric collisions alone, such that other loss processes are clearly dominant. For example, one important loss process is driven by whistler-mode waves, including plasmaspheric hiss, lightning-generated whistlers, and man-made transmissions [Abel and Thorne, 1998; Rodger *et al.*, 2003].

[5] It has been recognized that HANEs would shorten the operational lifetime of Low Earth Orbiting satellites [U.S. Congress, 2001; Steer, 2002], principally owing to the population of HANE-injected >1 MeV trapped electrons. It has been suggested that even a "small" HANE (~ 10 – 20 kilotons) occurring at altitudes of 125–300 km would raise peak radiation fluxes in the inner radiation belt by 3–4 orders of magnitude, and lead to the loss of 90% of all low-Earth-orbit satellites within a month [Dupont, 2004]. In the event of a HANE, or an unusually intense natural injection, this large population of valuable satellites would be threatened. Owing to the lifetime of the injected electrons, the manned space program would need to be placed on hold for a year or more. However, recent theoretical calculations have led to the rather surprising conclusion that wave-particle interactions caused by man-made very low frequency (VLF) transmissions may dominate non-storm time losses in the inner radiation belts [Abel and Thorne, 1998]. This finding has sparked considerable interest, suggesting practical human control of the radiation belts [Inan *et al.*, 2003] to protect Earth-orbiting systems from natural and man-made injections of high-energy electrons [Rodger *et al.*, 2006]. This man-made control of the Van Allen belts has been termed "Radiation Belt Remediation" (RBR).

[6] Satellite observations of quasi-trapped ~ 100 keV electrons in the drift-loss cone have reported "spikes" or enhancements in the flux population associated with the geomagnetic locations of VLF transmitters [see Datlowe and Imhof, 1990; Datlowe, 2006, and references therein].

Enhancements of drift-loss cone electron fluxes are expected eastward of the transmitter location, with cyclotron resonance taking place on field lines near the ground-based VLF transmitter, followed by the eastward drift of electrons toward the South Atlantic Anomaly. Transmitters located under a nighttime ionosphere are likely to be more effective, owing to the lower ionospheric absorption of the up-going transmitter waves. Proposed RBR systems have not focused upon ground-based VLF transmitters, but they can serve as a test bed for examining the effectiveness of man-made control systems, and increasing our understanding of the wave-particle interactions which are likely to underpin an operational RBR system.

[7] Very recently, observations by the Detection of Electro-Magnetic Emissions Transmitted from Earthquake Regions (DEMETER) microsatellite near the powerful VLF transmitter NWC have shown that this transmitter causes electron and ion heating in the ionosphere at 700 km, affecting a $\sim 500,000$ km² region [Parrot *et al.*, 2007]. These authors also presented DEMETER-measured increases in energetic electrons in the range 91–527 keV, attributed to NWC. Following on from this study, a further examination of DEMETER wave and particle data considered the significance of NWC upon electrons in the inner radiation belt, showing that enhancements in the ~ 100 – 600 keV drift-loss cone electron fluxes at low L values are linked to NWC operation and to ionospheric absorption [Sauvaud *et al.*, 2008]. The enhancements, termed "wisps," are only detected eastward of the transmitter location, as expected from the electron drift motion, and at energies that are consistent with first-order equatorial cyclotron resonance between the NWC transmissions and electrons interacting in the vicinity of the magnetic equatorial plane. These authors conclude that the NWC transmitter is extremely well positioned to have a potential influence upon inner radiation belt >100 keV electrons.

[8] Some previous authors have argued that nonducted propagation will play an important role in electron precipitation driven by ground-based VLF transmitters [Inan *et al.*, 2007], as non field-aligned propagation allows high-order resonances hence driving the loss of higher-energy particles. It is generally accepted that there is no significant ducting below $L = 1.6$ as the plasmaspheric electron density increases which cause ducting are not sufficient below this point. Recently, Clilverd *et al.* [2008] concluded that the transmissions from a VLF transmitter located in Hawaii were wholly nonducted as they propagated through the inner plasmasphere. However, the same study found that the conjugate wave power from NWC stretched from $L = 1.4$ to $L = 2.2$, arguing that the dominant propagation mechanism for $L = 1.4$ to $L = 1.6$ is nonducted, while ducted propagation dominates for $L > 1.6$.

[9] In this paper we expand upon the earlier Sauvaud *et al.* [2008] letter to provide additional details as to the effect of transmissions from NWC on inner radiation belt electrons. Specifically we examine the occurrence frequency of drift-loss cone enhancements observed above transmitters, the intensity of the flux enhancements, and clearly demonstrate the linkage to transmitter operation. In addition, we consider the relative effectiveness of ducted and nonducted

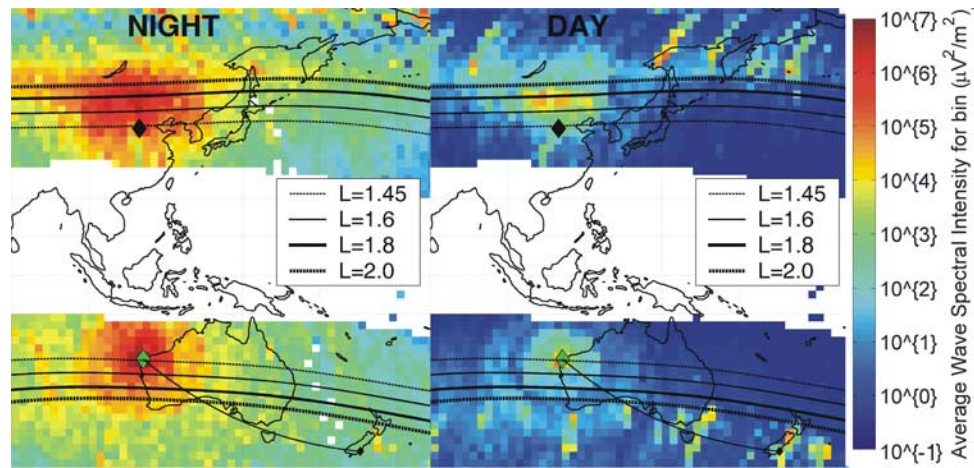


Figure 1. Average power received by the Instrument Capteur Electrique (ICE) on Detection of Electro-Magnetic Emissions Transmitted from Earthquake Regions (DEMETER) at 19.8 kHz for (left) night orbits and (right) day orbits. The locations shown are those found by tracing from the satellite down the field line to 100 km altitude. The subionospheric path from transmitter NWC to Dunedin is shown, as are L -shell contours. The dark diamond in the Northern Hemisphere indicates the conjugate location of the transmitter.

propagation on pitch angle scattering of inner radiation belt electrons.

2. Instrumentation

[10] DEMETER is the first of the Myriade series of microsatellites, and was placed in a circular Sun-synchronous polar orbit at an altitude of 710 km at the end of June 2004. Data are available at invariant latitudes $<65^\circ$, providing observations around two local times (~ 1030 LT and 2230 LT). The Instrument Detecteur de Particules (IDP) carried on board DEMETER looks perpendicularly to the orbital plane of the satellite, and thus detects fluxes of $\sim 90^\circ$ pitch angle electrons inside, or just outside, the drift-loss cone. This instrument is unusual in that it has very high energy resolution; in normal “survey” mode the instrument measures electron fluxes with energies from 70 keV to 2.34 MeV, using 128 energy channels every 4 s [Sauvaud *et al.*, 2006]. Energy resolution depends on the operational mode of the satellite, being either 17.8 keV in “survey” mode or 8.9 keV in “burst” mode. All burst-mode data we consider in our study were down-sampled to survey-mode resolution in this study for homogeneity. The same spacecraft also carries the Instrument Capteur Electrique (ICE), which provides continuous measurements of the power spectrum of one electric field component in the VLF band [Berthelier *et al.*, 2006]. Here we make use of both survey- and burst-mode data of the electric field spectra recorded up to 20 kHz, with a frequency channel resolution of 19.25 Hz.

[11] In addition, we also make use of narrowband sub-ionospheric VLF data received at Dunedin, New Zealand (45.9°S , 170.5°E) by an OmniPAL receiver, part of the Antarctic-Arctic Radiation-belt Dynamic Deposition VLF Atmospheric Research Konsortia (AARDDVARK). More information on AARDDVARK can be found at the following Web site: http://www.physics.otago.ac.nz/space/AARDDVARK_homepage.htm.

[12] The powerful U.S. Navy transmitter with call sign “NWC” (19.8 kHz, 1 MW radiated power, North West Cape, Australia, $L = 1.45$) is extremely well positioned to have a potential influence upon >100 keV electrons in the inner radiation belt; most other powerful VLF transmitters are located at much higher L shells, leading to resonances with <10 keV electrons. Figure 1 (left) shows the average spectral power received by DEMETER’s ICE instrument in a ~ 195 Hz band centered on 19.8 kHz, for nighttime orbits occurring from 12 August to 26 September 2005. Throughout our study, DEMETER satellite locations are specified in geographic coordinates, which have been traced down the magnetic field line to an altitude of 100 km using the IGRF-2000 model, epoch 2005. Figure 1 suppresses data coverage near the geomagnetic equator as the results of the field tracing becoming incorrect at very low latitudes. The location of NWC is shown by a dark diamond, and the subionospheric great circle path from NWC to Dunedin is also marked. In the DEMETER data, NWC produces high power levels in both the source and conjugate hemispheres, although the conjugate location is shifted poleward as discussed by Clilverd *et al.* [2008] owing to nonducted propagation through the plasmasphere. Figure 1 (right) shows the average spectral power received from NWC for daytime orbits during the same time period. As can be seen in Figure 1, DEMETER also clearly observes NWC transmissions during the day in the same time period, but at power levels which are typically ~ 1200 times (i.e., ~ 31 dB) lower owing to increased ionospheric absorption. This is reasonably consistent with the ~ 37 dB difference between the estimated daytime and nighttime ionospheric absorption for a 20 kHz signal [Helliwell, 1965, Figure 3–35]. For short-lived electromagnetic wave events, like whistlers, the pitch angle scattering efficiency is proportional to whistler-mode wavefield amplitude rather than power [e.g., Chang and Inan, 1983]. However, in the case of a long-lasting electromagnetic wavefield produced from a continuously operating VLF transmitter, particles bounce (and interact with the

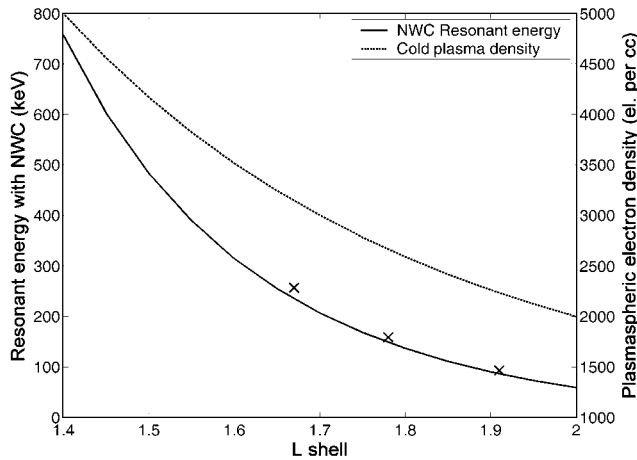


Figure 2. Typical UT variation in transmissions from the VLF station NWC, received at Dunedin, New Zealand, 21–27 August 2005. Nighttimes correspond to the periods with higher amplitudes. This plot presents 1-min average amplitudes, demonstrating the near-constant operation of this transmitter.

waves) many times while crossing the illuminated region, and while each individual pitch angle change is proportional to field amplitude, there is a random phase so the cumulative effect is roughly diffusive. In this case the scattering “efficiency” should scale linearly with power, suggesting that the transmissions from NWC should be ~ 1200 times more effective at scattering energetic electrons toward the loss cone during local nighttime.

[13] Subionospheric signals from NWC received at Dunedin are >40 dB above the noise floor, allowing us to use these observations to confirm NWC on and off periods. Figure 2 shows the UT typical variation in NWC transmissions received in Dunedin, in this case shown in the form of 1-min-average amplitudes measured from 21 to 28 August 2005. The typical diurnal amplitude variation spans 15–16 dB, with smoothly varying amplitudes during the period where the lower edge of the ionosphere is illuminated by the Sun, and higher amplitudes during the night. During the daytime period of 22 August the transmitter did not broadcast for ~ 7 h, and the amplitude drops by ~ 50 dB down to the noise floor. This is the weekly maintenance period for this transmitter and reflects the pattern of operation of U.S. Navy transmitters during normal operations, that is, near-constant broadcasting (roughly 95% of the time).

3. Drift-Loss Cone Observations

[14] Particle measurements by the IDP instrument were examined for DEMETER orbits in the time period 12 August to 26 September 2005 when the spacecraft passed within $\pm 25^\circ$ longitude of NWC’s location. While our time period included significant geomagnetic storms [e.g., Rodger et al., 2007a], IDP observations indicate that these storms did not produce significant radiation belt electron flux enhancements at $L < 2$. For clarity, only observations taken when DEMETER was located in NWC’s hemisphere (i.e., the Southern Hemisphere) were consid-

ered. Under these constraints there were 173 half-orbits examined, of which 84 were for nighttime conditions, that is, when the ionosphere is not illuminated by the Sun. A significant number of the orbits contain enhancements of drift-loss cone electron fluxes with a characteristic pattern; throughout this study we will term such enhancements “wisps,” following Sauvaud et al. [2008]. A set of four typical wisps are shown in Figure 3, presenting the IDP instrument-measured differential electron fluxes in units of electrons $\text{cm}^{-2} \text{s}^{-1} \text{sr}^{-1} \text{keV}^{-1}$ during these events. The four examples present wisps on 27 August 2005 (starting at 1359 UT, 14.2 min long, 24° east of NWC), 3 September 2005 (1315 UT, 13.9 min, 22° east), 4 September 2005 (1359 UT, 14.0 min, 12° east), and 20 September 2005 (~ 0359 UT, 14.1 min, 12° east). The wisp features are very clear in these passes; for example, on 27 August 2005 the wisp is the feature which starts at $L \approx 1.6$ and ~ 350 keV, and decreases in energy with increasing L , as expected from cyclotron resonance [e.g., Chang and Inan, 1983]. The enhanced electron flux seen in all examples for $L > 2$ is a consistent feature associated with the energy structure of the radiation belts. Both the features of our wisps and the energy structure in the inner radiation belt are essentially the same as those shown in Figure 1 of Datlowe [2006], where the single “wisp” shown was attributed to field-aligned, first-order, cyclotron resonance with transmissions from NWC.

[15] Table 1 summarizes our observations of wisps comparing occurrence rates to the west and east of NWC and also separated into nighttime and daytime orbits. The first value given in each cell of Table 1 is the number of half-orbits examined, while the second value gives the number of those half-orbits that have been observed to contain wisps. Clearly, the vast majority of wisps are observed in the orbits which are within 25° east of NWC. Additionally, wisps are observed only during nighttime half-orbits, almost certainly owing to the much lower ionospheric absorption of NWC transmissions through the nighttime ionosphere. Of the three eastern nighttime half orbits for which no wisp was observed, NWC was not transmitting for one of these times, although was transmitting for the other two times. Thus for nighttime conditions, DEMETER observations show that when broadcasting NWC creates “downstream” drift-loss enhancements of >100 keV electrons $\sim 95\%$ of the time, but is unable to produce a significant effect under a daytime ionosphere. These enhancements will drift around the Earth to the South Atlantic Anomaly, where they will precipitate into the atmosphere. A small number of wisps were observed during nighttime orbits occurring west of NWC ($\sim 22\%$ of the time), with all but one of these wisps occurring within 6° longitude of the transmitter. Although less common this is consistent with an NWC-driven scattering mechanism, as the longitudinal extent of the NWC transmissions is significant, as shown in Figure 1. VLF transmitters located westward of NWC, for example in Europe are unlikely to be the source of those wisps observed slightly to the west of NWC’s location. European transmitters are located conjugate to the eastern edge of the South Atlantic Anomaly, and hence any electrons undergoing pitch angle scattering from these transmitters are likely to be driven into the local bounce loss cone and lost immediately into the conjugate atmosphere. In addition, Figure 2 of Sauvaud et al. [2008] shows no significant

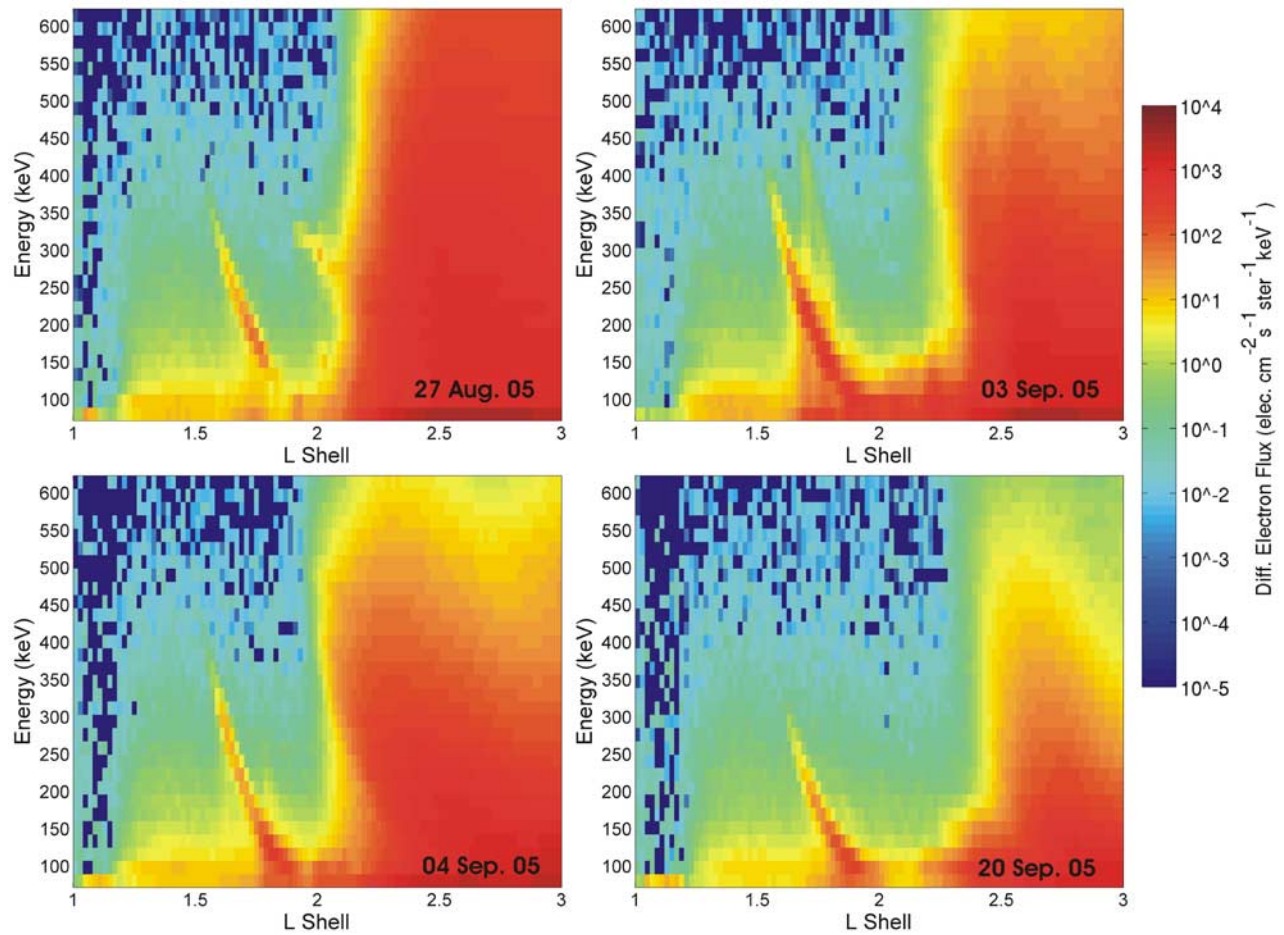


Figure 3. Examples of typical drift-loss cone electron flux enhancements, termed wisps, seen from $L = 1.6$ – 1.8 in the Instrument Detecteur de Particules (IDP) observations during a DEMETER orbit. Four examples are given of the absolute flux measurements in units of electrons $\text{cm}^{-2} \text{s}^{-1} \text{sr}^{-1} \text{keV}^{-1}$ during wisp events.

enhancement in the 200 keV fluxes to the west of NWC's location, and an enhancement which stretches from NWC's approximate location eastward to the South Atlantic Anomaly.

4. Wisp Event Link to NWC Operation

[16] During the 12 August to 26 September 2005 study period selected, NWC generally operated in its normal mode of near-continuous broadcast punctuated by regular ~ 7 h maintenance periods (Figure 2). In general, it is very rare for NWC to be nonoperational during local nighttime.

Table 1. Summary of Wisp Observations at 25° Longitude West of NWC and at 25° Longitude East of NWC, Observed During Nighttime or Daytime Orbits^a

	Day	Night
East	(43) 0	(39) 36
West	(46) 0	(45) 10

^aThe first value given is the number of half-orbits examined; the second gives the number of those half-orbits containing wisps.

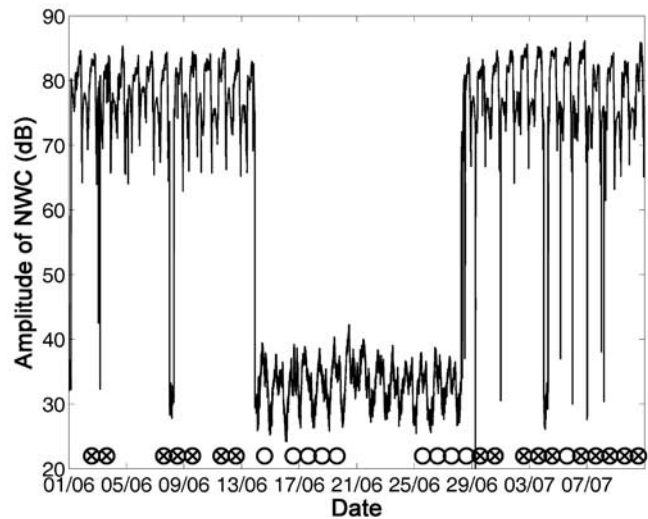


Figure 4. Dunedin-received 1-min average NWC amplitudes in June 2005 during a period in which NWC ceased transmitting for ~ 14 days. The circles indicate the times DEMETER nighttime orbits were within 25° eastward of NWC, while the crossed circles show orbits in which wisps were observed.

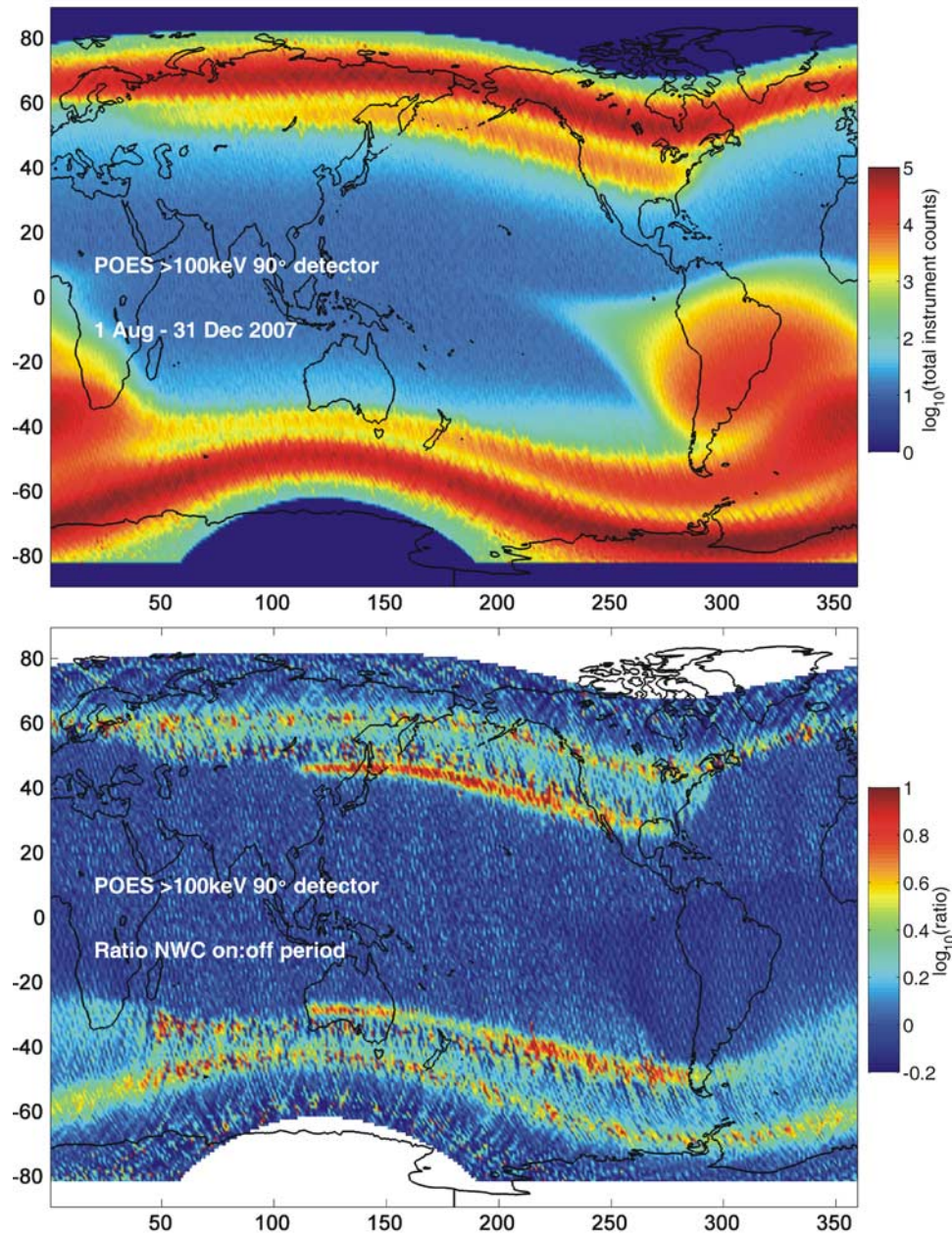


Figure 5. The effect of the NWC transmissions seen in the >100 keV electron observations from the Polar Orbiting Environmental Satellites (POES) spacecraft. (top) The sum of all the >100 keV electron counts from the Medium Energy Proton and Electron Detector (MEPED) 90° detector for the period 1 August to 31 December 2007 when NWC was not operating. (bottom) The ratio between the period 1 January to 31 May 2007 and the top image. NWC was operating normally in the first half of 2007.

However, subionospheric measurements of NWC received at Dunedin show that NWC was not transmitting throughout the period from ~2200 UT on 13 June 2005 through to 0618 UT on 28 June 2005 (Figure 4). Over this time period, there were eight nighttime DEMETER half-orbits within 25° longitude eastward of NWC. None of these orbits showed wisps in the drift-loss cone fluxes. The circles marked in Figure 4 indicate the times of DEMETER nighttime orbits east of NWC, while crossed circles show orbits in which wisps were observed. Wisps were seen immediately before, and after, the NWC off time period,

when NWC was transmitting normally. These observations provide conclusive evidence of the linkage between wisps and transmissions from NWC.

[17] As an additional test, we examine the long-term observations of inner radiation belt electrons in 2007. From 1 July 2007 through to about 22 January 2008, NWC did not transmit. Figure 5 shows a world map of the combined >100 keV electron counts from the 90° electron telescopes on the NOAA 15, 16, 17, and 18 Polar Orbiting Environmental Satellites (POES) spacecraft for the time period 1 August to 31 December 2007. The latitude and longitude

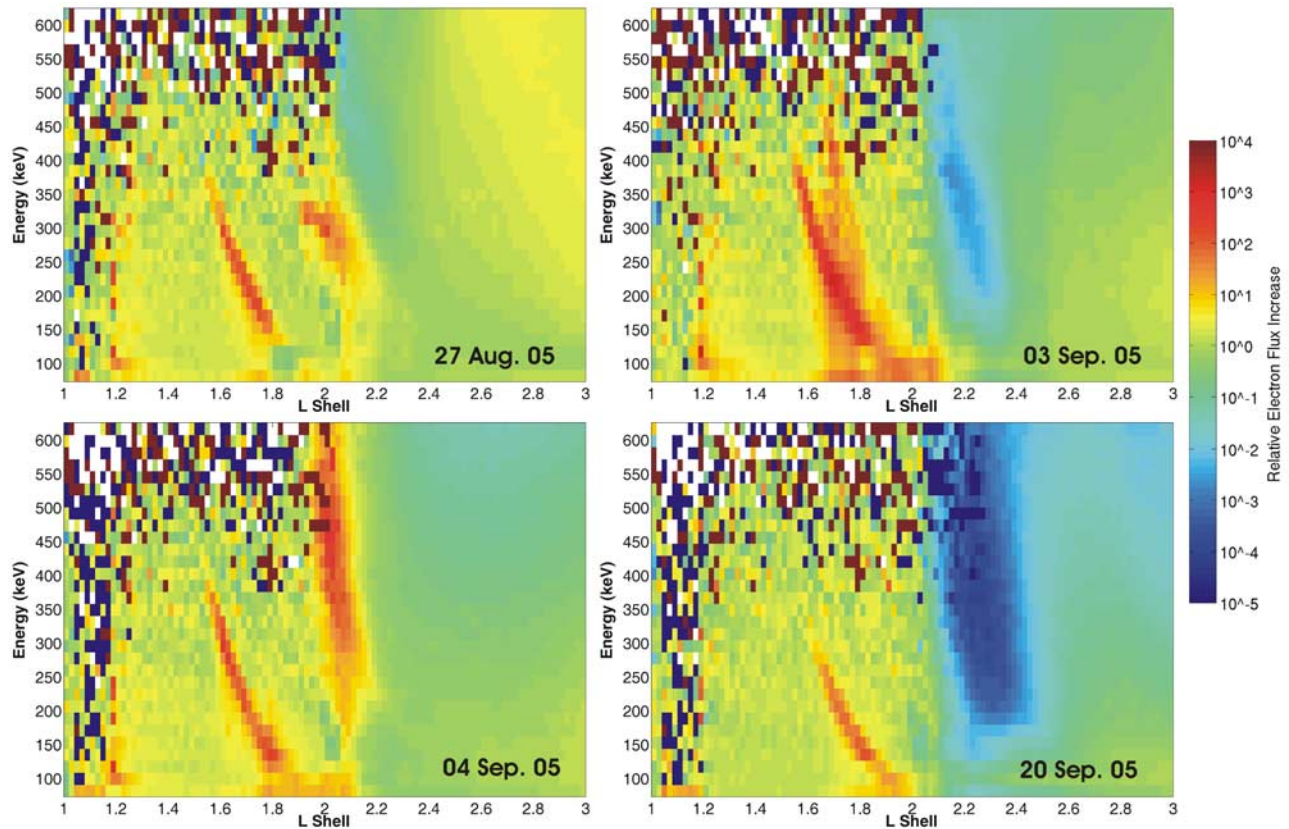


Figure 6. Examples of the relative electron flux enhancements for the four wisp events shown in Figure 3. The wisp enhancements are shown relative to a reference background spectrum when NWC was not transmitting and no wisp enhancement was present.

shown is the geographic position of the subsatellite point. In order to increase the sensitivity of our test, we combine all the 16 s electron integral flux observations provided by NOAA's National Geophysical Data Center, by summing the observations for all times in that period from all the satellites, with 1 degree resolution. The 90° electron telescope of the Medium Energy Proton and Electron Detector (MEPED) instrument detects trapped and quasi-trapped electrons in the inner radiation belt. This can be seen from Figure 5 (top), where the inner belt fluxes increase considerably from $\sim 75^\circ\text{E}$ eastward to $\sim 250^\circ\text{E}$. This image shows the expected structure of the radiation belts, with the inner and outer belts separated by the slot region, and the South Atlantic Magnetic Anomaly. NWC operated normally in the first part of 2007. Figure 5 (bottom) shows the ratio between the period 1 January to 31 May 2007, when NWC was broadcasting normally and the period 1 July to 31 December 2007 (Figure 5, top) when NWC was off. The POES-observed >100 keV electron fluxes increase by ~ 5 – 7 times from the longitude of NWC through to the South Atlantic Magnetic Anomaly, owing to the operation of NWC. This difference is more significant than the variation in slot region fluxes, likely to be due to seasonal variations in plasmaspheric hiss occurrence and plasmaspheric densities.

[18] We have also examined the MEPED >100 keV 0° electron telescope observations. At NWC latitudes this should be measuring electrons in the bounce loss cone. However, we do not see any indication of enhanced bounce

loss cone fluxes around NWC. This is likely to be due to the sensitivity of the instrument, as the expected distribution of whistler-generated electron precipitation [Rodger *et al.*, 2007b] is also not present in this data, which is likely to be more intense in some regions than the NWC-driven losses into the bounce loss cone.

5. Relative Electron Flux Enhancements in Wisp Events

[19] In order to examine the magnitude of wisp events they are compared to the electron flux observed by DEMETER across the same L -shell range on 29 August 2005 from 1436 to 1449 UT. NWC was not transmitting in this time period, and this is one of the 3 nighttime orbits east of NWC for which no wisp was present. We use these fluxes to provide an indication of the undisturbed electron drift-loss electron fluxes, and thus to determine the significance of NWC-driven scattering. An example of this is shown in Figure 6, where the relative flux enhancements are presented for the four wisp events shown in Figure 3. In the L -shell range below $L = 2$, there is generally agreement between the electron densities measured outside the wisp features and the “nondisturbed” fluxes from 29 August 2005. Above $L = 2$ there can be differences of several orders of magnitude, due to variations in the fluxes in the electron slot region. The four examples of Figure 6 are representative of wisp events observed. Typically, the wisp flux values in a single

Table 2. Summary of Typical Wisp Properties for the 46 Events Observed in August to September 2005^a

	Lower L	Mid L	Upper L	Lower E (keV)	Mid E (keV)	Upper E (keV)	Flux Enhancement
Mean	1.67	1.77	1.90	103	168	262	429
Median	1.67	1.78	1.91	93	159	257	175

^aThe peak flux enhancement is the relative increase factor in the quasi-trapped electron fluxes.

event are approximately at a constant multiplicative value above the background quasi-trapped electron fluxes in the drift-loss cone. This implies that the efficiency of the pitch angle scattering mechanism that produces wisps is linear in both energy and L range. Table 2 provides a summary of the typical L shell, energy range, and enhancement factor for the 46 wisps observed in the August to September 2005 period. Typically, the wisps extend from $L = 1.67$ – 1.9 , although the upper L cutoff is likely to be limited by the lower-energy threshold for the IDP instrument. Wisp events can have a fairly varied upper energy, ranging from ~ 120 – 410 keV, and also a wide range of enhancement factors, with the peak flux enhancement ranging from ~ 1.2 times to 2200 times the reference spectrum with a (geometric) mean enhancement factor of ~ 430 . Thus, there are typically ~ 430 times more 100–260 keV resonant electrons present in the drift-loss due to NWC transmissions compared with periods when NWC is nonoperational.

[20] After the 13–28 June 2005 NWC off time period, one might expect the wisp enhancements to be larger, owing to a buildup in fluxes during the off time. No such difference is observed in the wisp flux levels once NWC resumes operation, although it is questionable if such an increase would be detectable when compared with the large variation in wisp enhancements during constant NWC operation. In addition, it should be noted that the first wisp observation after the transmitter's nonoperational period occurs at 1327 UT on 29 Jun 2005, ~ 31 h after the transmitter resumes operation. Compared to the electron drift period of ~ 4 – 5 h in this energy and L shell range (once around the Earth), it is more likely than any increase in wisp enhancements due to this effect will have been “flushed out” such that it is not discernable in this data set by the time the craft has the opportunity to measure it.

[21] The significance of the NWC loss cone enhancements has been estimated through comparison with the AE-5 Inner Zone Electron Model [Teague and Vette, 1972]. This model provides analytic functions for the unidirectional differential energy flux and is based on data collected during solar maximum conditions. The analytic functions in AE-5 describe quiet-day electron fluxes for $1.3 \leq L \leq 2.4$ and are based on observations of electrons with $E < 690$ keV. Transmissions from NWC typically scatter into the drift-loss cone roughly 0.05% of the AE-5 described electrons with resonant energy (i.e., $E = 168$ keV at $L = 1.77$) in a magnetic flux tube with 1 cm^2 square cross section at 100 km. In contrast, a 0.5–10 kHz whistler will typically scatter 0.005% of the resonant electrons of a given energy into the bounce loss cone (following the approach of Rodger *et al.* [2003]). However, we note that this is not a

like with like comparison, as the resonant energies for the whistler at $L = 1.77$ span 330–2900 keV.

6. Comparison With Cyclotron Resonance Calculations

[22] Figure 7 shows the predicted variation with L of the first-order cyclotron resonant energy for energetic electrons resonant at the geomagnetic equator with 19.8 kHz waves (solid line), determined from the expressions of Chang and Inan [1983]. The resonant energy is strongly dependent upon the plasmaspheric electron density, shown in Figure 7 by the dotted line. The plasmaspheric electron densities used were interpolated using two sets of experimental observations from $L = 2.2$ and $L = 1.4$. The higher L -shell measurements come from the ISEE 1 satellite and whistler-based mid-solar-cycle results of Carpenter and Anderson [1992]. The lower L -shell measurements come from the Alouette-2 satellite results of Mahajan and Brace [1969] near $L = 1.4$ (altitudes ~ 2500 km) for the period May 1966 to March 1967. In Figure 7 the crosses show the median wisp values for L and energy from Table 2. Thus there is very good agreement between the calculations and a typical wisp, providing additional evidence that the wisps are generated by first-order cyclotron resonance with 19.8 kHz waves from NWC, with the interaction taking place at or near the geomagnetic equator. The lowest energy of the NWC-generated wisps is close to the lowest energy channel

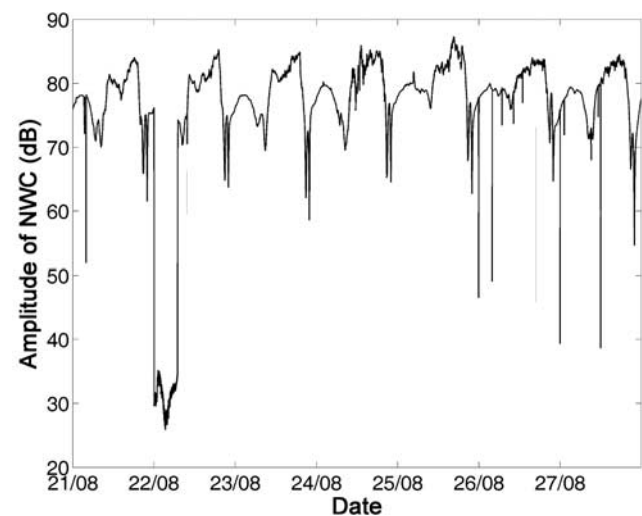


Figure 7. Variation with L of the first-order cyclotron resonant energy with waves of 19.8 kHz (solid line) and the plasmaspheric electron number density used in this calculation (dashed line). The crosses mark the mean L and energy for typical wisps as described in Table 2.

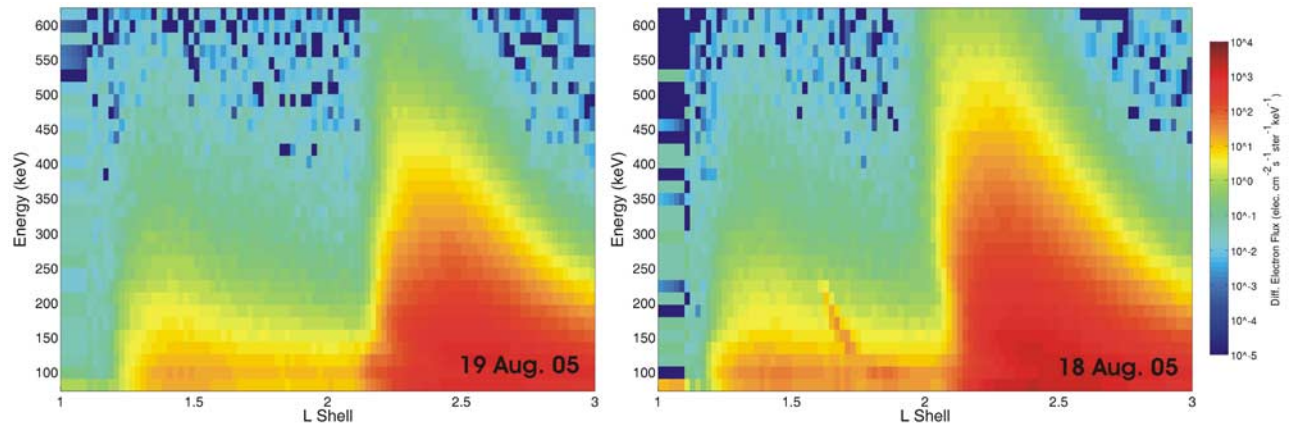


Figure 8. Examples of DEMETER IDP observations east of the VLF transmitter NPM at night. (left) The typical situation, where no wisp is present. (right) A rare observation of a wisp likely generated by ducted transmissions from NPM.

observed by the IDP instrument, so that enhancements at higher L shells will be below this energy floor. The lower L and upper energy limits are likely to be due to the propagation mode of NWC through the plasmasphere, as discussed in section 5. A similar high-quality fit between resonant energy calculations and a wisp event [Sauvaud *et al.*, 2008, Figure 3] was determined using a totally different plasmaspheric electron density model, indicating the robustness of these calculations.

7. Comparison With Other VLF Transmitters

[23] Clearly NWC produces a very strong feature in the quasi-trapped electron fluxes for energies of a few hundred keV and in the L -shell range of ~ 1.67 to ~ 1.9 , which is well predicted by first-order cyclotron resonance. It is interesting to consider whether DEMETER can observe drift-loss cone enhancements produced by other VLF transmitters. As noted above, VLF transmitters in Europe lie in the conjugate region to the eastern edge of the South Atlantic Anomaly, and hence will not lead to an enhancement in drift-loss cone electrons, as any electrons will be driven into the local bounce cone and lost immediately into the conjugate atmosphere. Should this be taking place, it would be challenging to detect in DEMETER observations. Similarly, the powerful U.S. Navy transmitter, NAA, on the east coast of the United States is conjugate to the western edge of the South Atlantic Anomaly. Assuming that the resonant energies will also be governed by first-order resonance, the L shells of NAA and the majority of the European transmitters suggest their transmissions will be resonant with relatively low energy electrons (< 100 keV), often below the lower cutoff for DEMETER IDP observations.

[24] One other possible transmitter candidate for producing significant detectable drift-loss enhancements (in addition to NWC) is the ~ 500 kW U.S. Navy communications station with call sign NPM broadcasting at 21.4 kHz from Hawaii ($L = 1.17$). Observations from the DEMETER spacecraft in the hemisphere conjugate to NPM indicate the transmitted power spreads across $L = 1.2$ to $L = 1.5$ [Clilverd *et al.*, 2008]. If the NPM transmissions interacted with inner radiation belt electrons through first-order reso-

nance, the resonant energies would be high, for example 700 keV at $L = 1.4$ and 450 keV at $L = 1.5$. We examined DEMETER orbits from 12 August to 26 September 2005 which passed within 25° longitude east of NPM in the Northern Hemisphere. During this time NPM was largely broadcasting in the standard U.S. Navy pattern of operation, and hence was operational near continuously. The majority of the 37 NPM orbits occurring in daylight contained wisps occurring over the same L shell and energy range as previously observed to be produced by NWC. At these times there was a nighttime ionosphere above NWC, and hence NWC wisp generation is expected, as NWC-generated wisps will drift to NPM's longitude in ~ 70 min or less, depending on energy. Conversely, when there was a nighttime ionosphere above NPM, NWC would be day lit, which removes the possibility of NWC-generated wisps. We examined 36 orbits eastward of nighttime NPM. Thirty-five of them showed no detectable enhancement in the quasi-trapped electron fluxes (i.e., no wisps). Figure 8 (left) shows a typical orbit from this period on 19 August 2005, starting at ~ 0734 UT. Even though NPM radiates roughly half the output power of NWC and thus might be expected to produce an enhancement at least 200 times the background, no wisp features are present in this case. In the L region from 1.2 to 1.5 where wisps might be expected owing to nonducted NPM transmissions, the quasi-trapped electron fluxes are ~ 10 times higher than for the orbits east of NWC shown in Figure 3, owing to the steady filling of the drift-loss cone with eastward drift. Nonetheless, the NWC-generated wisps are still clear in the NPM daytime orbit data, and thus we would expect evidence for nonducted NPM-generated wisps despite the higher background levels. Only one of the nighttime orbits east of NPM contains a wisp, occurring across the L range 1.6 to 1.725 as shown in Figure 8 (right). This single wisp event is consistent with ducted NPM propagation leading to an enhancement around 190 keV at $L = 1.7$, as outlined below.

[25] As noted above, transmitters at $L < 1.6$ will propagate through the plasmasphere in a nonducted manner, while those beyond appear to be largely ducted [Clilverd *et al.*, 2008]. This study indicated that NPM transmissions were largely nonducted, and argued that the transmissions

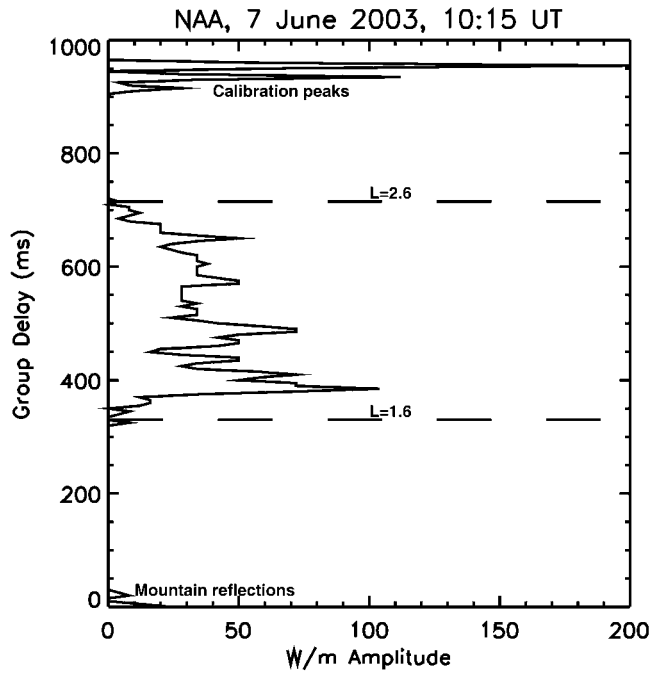


Figure 9. Amplitude of received NAA whistler-mode signals arriving at Rothera (Antarctica) as a function of group delay time. The group delays, which are typical of nighttime ducted propagation, have L values in the range $L = 1.6$ – 2.6 (as shown by two horizontal dashed lines). Also shown on the plot are subionospheric mountain reflections, which have very little delay compared with the arrival time of the direct, subionospheric signal.

from NWC would be nonducted from $L = 1.4$ to $L = 1.6$ and ducted up to $L = 2.2$ (the highest L shell for which conjugate transmissions from NWC were observed). The resonance energies for NWC-generated wisps are consistent with solely first-order field-aligned resonance starting at $L = 1.6$, that is, consistent with ducted propagation starting at this L shell. Nonducted propagation leads to significantly higher resonance energies than first-order resonances for field-aligned propagation. *Datlowe and Imhof* [1990] found the resonance energy almost doubled as the angle changed from 0° (field aligned) to 70° . The lack of any wisp enhancement for $L < 1.6$ suggests that nonducted propagation is an inefficient mechanism for scattering electrons, which explains the lower cutoff in L of the NWC-generated wisps and the lack of NPM-generated wisps. Calculations of >100 keV electron precipitation from ground-based transmitters based on nonducted propagation through the magnetosphere predicts that the >100 keV flux due to NWC at $L = 1.7$ should be only 25% higher than that due to transmissions from NPM [Kulkarni *et al.*, 2008]. This study also suggests that the peak in NWC-driven scattering of >100 keV electrons should lie at about $L = 2$, which is outside the range of the wisp events observed in DEMETER, and inconsistent with the observations reported in the current study. In practice it is not clear in the DEMETER data that there is any nonducted electron scattering from either transmitter, with the single NPM scattering event observed consistent with a ducted

wave, despite the small differences expected from nonducted calculations.

[26] While Figure 1 shows there is somewhat less power from NWC observed at DEMETER in the $L = 1.4$ – 1.6 conjugate region when contrasted with $L = 1.6$ – 1.8 , our observed wisps start suddenly at $L \approx 1.6$ (where ducting starts). This implies that NWC is one of the few transmitters for which there will be regular scattering of >100 keV electrons which can be easily detected by satellites as they drift around the Earth. The Italian VLF transmitter (40.9°N , 9.8°E , $L = 1.45$) should produce significant ducted signals, but owing to its location near the anomaly these transmissions will scatter electrons directly into the local bounce loss cone. In contrast, the Indian transmitter (8.45°N , 77.75°E , very near the magnetic equator) and Japanese transmitter (32°N , 130.8°E , $L = 1.23$) will be much like NPM, rarely coupling into ducts and thus not producing significant scattering due to their nonducted propagation through the plasmasphere. The majority of the remaining VLF transmitters are at higher L , and hence the transmissions from these transmitters will resonant with lower-energy electrons.

[27] If the NWC-generated wisps are produced solely by ducted propagation of NWC through the plasmasphere, it is reasonable to question if ducts are large enough to span from $L = 1.6$ to at least $L = 1.91$, and also whether ducts might be expected to be present at longitudes very close to NWC $\sim 95\%$ of the time. An effective method of testing this idea is to use data from a ground-based experiment that monitors the signals produced by a large VLF transmitter similar to NWC that have propagated through the plasmasphere as ducted whistler-mode waves. Well-located, near-conjugate, observations of whistler-mode signals from the powerful U.S. Navy VLF transmitter in Cutler, Maine (NAA, 24.0 kHz), have been made in Antarctica almost continuously since 1986 [Clilverd *et al.*, 1991, 2000]. For more than two solar cycles close to 100 percent of nights have shown one-hop whistler-mode signals when the transmitter has been on. Recordings have been made such that multihop whistler modes could be observed, although to date none have been detected. This suggests that multihop whistler-mode signals from VLF naval transmitters are very rare, which is consistent with the lack of wave amplification of NAA whistler-mode signals reported by Clilverd and Horne [1996]. Hence we conclude that the DEMETER-observed wisps are likely due to the interaction with primarily one-hop whistler-mode transmitter signals.

[28] Figure 9 shows a typical example of nighttime whistler-mode signals received at Rothera station, Antarctica (67.5°S , 68.1°W , $L = 2.7$), due to transmissions from NAA. This transmitter has a very similar output power to NWC. The plot shows the amplitude of received NAA whistler-mode signals arriving at Rothera as a function of group delay time. The group delays are indicative of nighttime ducted propagation between $L = 1.6$ and $L = 2.6$ as indicated by two horizontal dashed lines. Also shown on the plot are subionospheric mountain reflections, which have very low delay compared with the arrival time of the direct, subionospheric signal [Thomson, 1989], and software calibration signals of known amplitude. A similar plot for NPM has been presented by Thomson [1987, Figure 4].

[29] The lower L -shell limit of the whistler-mode signals at $L = 1.6$ in Figure 9 is consistent with the ducted whistler-mode propagation seen in Figures 3, 5, 6, and 8 of the current study, and the upper limit at $L = 2.6$ is consistent with the half-gyrofrequency cutoff for interhemispheric ducted propagation [Clilverd *et al.*, 2008]. From the data in Figure 9 we can see that although individual ducts are present across many L shells (group delays), there is a general spread of whistler-mode power in the range $1.6 < L < 2.6$, and of particular interest here, across $L = 1.67\text{--}1.9$, which can explain the uniform L -shell spread of NWC-generated wisp flux enhancements observed by DEMETER. Long-term studies of NAA from the Antarctic Peninsula have also shown that ducts are observed at longitudes close to the transmitter almost every night of the year [Clilverd *et al.*, 1993], which would be consistent with the 95% NWC wisp occurrence rate observed. It seems possible that the ionospheric heating produced by the VLF transmitter, as has been reported over NWC [Parrot *et al.*, 2007], may itself lead to the production of ducts above the transmitter. This deserves further modeling.

8. Discussion

[30] The U.S. Air Force is to launch the Demonstrations and Science Experiment (DSX) mission in 2009, which will include the Radiation Belt Remediation experiment with a 50 m antenna to [Winter *et al.*, 2004, p. 531] “demonstrate the viability of VLF RBR techniques.” The VLF payload of this mission is to include a transmitter to broadcast up to the kilowatt level in the range 1–50 kHz. The power of the NWC transmissions received by DEMETER during the night at the transmitter’s latitude falls off as the longitudinal difference between the spacecraft and the transmitter increases, as expected. When contrasted with the signal powers calculated by the LWPC propagation model [Ferguson and Snyder, 1990] at the equivalent locations but below the night time ionosphere, we find the DEMETER observations are approximately 1000 times lower than those occurring below the ionosphere. In addition, the power of the DEMETER received nighttime NWC transmissions is observed to vary by about 2 orders of magnitude at the same location but from orbit to orbit. This is likely to be the primary reason for the large variations in the mean enhancement factor observed in wisps. Thus it appears that absorption decreases the power of NWC transmissions during the nighttime by $10^2\text{--}10^4$ times. As such NWC is roughly equivalent to a $\sim 0.1\text{--}10$ kW space-based transmitter during night periods, and a $\sim 0.1\text{--}10$ W transmitter during the day. Clearly, the transmissions from NWC provide an additional and potentially useful route for testing RBR systems, while the RBR-instrument onboard DSX is likely to produce smaller enhancements in the drift-loss cone fluxes than those due to the nighttime transmissions from NWC.

[31] The mostly likely causes for the large variations in the wisp mean enhancement factor are variations in the power of the NWC reaching the geomagnetic equator, or variations in the inner radiation belt trapped electron population having pitch angles just above the loss cone. Considering the first possibility, as mentioned above there is a very significant variation in the power of NWC received

at DEMETER during nighttime orbits, which should directly affect the rate at which particles are scattered into the loss cone. There is not a direct relationship between the DEMETER observed wisp enhancement and the DEMETER observed NWC power. However, the locations where DEMETER observes a wisp is normally considerably eastward from the longitudes where the wave-particle interactions are taking place (i.e., very near to NWC). As such the DEMETER observations are not well suited to test this. In contrast, the DSX observations will be well suited for such a test. Considering the second possibility, the IDP DEMETER instrument measures electrons in the drift-loss cone, and as such is not well suited for examining relationships between the wisp enhancement factor and trapped electron flux levels. While one might argue that there should be a relationship between the fluxes just inside and just outside the drift-loss cone, we do not find any relationship between the wisp enhancement factors and DEMETER observed nonwisp drift-loss cone fluxes (i.e., for energies just outside those of the wisp). In addition, it is likely that NWC will cause significant resonant scattering at pitch angles far from the loss cone, which will contribute to the long-term loss rate. This will alter the pitch angle distribution of the trapped electrons, and deserves further study. As another example of the effect of NWC on the inner radiation belts, we examined the >100 keV quasi-trapped electron fluxes (those in and near the drift-loss cone) observations from the four POES spacecraft in the range $L = 1.6\text{--}1.8$ varied by a factor of 20 during a 5 month period in which NWC did not operate. The variation was considerably higher outside this time period (peak variations of ~ 500 times). However, the August to September 2005 wisp enhancements do not track with the POES-observed variations, and it is not clear that these parameters observed by the DEMETER and POES are linked.

9. Summary and Conclusions

[32] Enhancements of drift-loss cone fluxes in the inner radiation belt have been observed to coincide with the geographic locations of the powerful VLF transmitter NWC. Sauvaud *et al.* [2008] demonstrated that enhancements in the $\sim 100\text{--}600$ keV drift-loss cone electron fluxes at low L values are linked to NWC operation and to ionospheric absorption producing enhancements, termed “wisps,” consistent with first-order equatorial cyclotron resonance. While proposed Radiation Belt Remediation systems have not focused upon ground-based VLF transmitters, studies into how these transmitters interact with inner radiation belt electrons can serve as a test bed for examining the effectiveness of man-made control systems, and increasing our understanding of the wave-particle interactions which are likely to underpin an operational RBR system. Sauvaud *et al.* [2008] concluded that the NWC transmitter is extremely well positioned to have a potential influence upon inner radiation belt >100 keV electrons. In this paper we have expanded upon the earlier study by examining the occurrence frequency of drift-loss cone enhancements observed above transmitters, the intensity of the flux enhancements, and by demonstrating the linkage to transmitter operation.

[33] Our study has confirmed that these drift-loss cone enhancements occur only at night. NWC signals received at the satellite during the day are at power levels which are typically ~ 1200 times lower than at night owing to the much higher ionospheric absorption, suggesting that nighttime transmissions from NWC should be ~ 1200 times more effective at scattering electrons. No energetic electron enhancements were observed during daytime periods, consistent with the increased ionospheric absorption. We have also confirmed the persistent occurrence of the wisp features east of the transmitter NWC. The enhancements can be observed within a few degrees west of NWC, and are present in 95% of the nighttime orbital data east of the transmitter for time periods when the transmitter is broadcasting. No enhancements are observed when NWC is not broadcasting. This provides conclusive evidence of the linkage between drift-loss cone electron flux enhancements and transmissions from NWC. When contrasted with periods when NWC is nonoperational, there are typically ~ 430 times more 100–260 keV resonant electrons present in the drift-loss cone across $L = 1.67$ – 1.9 due to NWC transmissions. Wisp events can have a fairly varied upper energy, ranging from 120 to 410 keV, and also a wide range of enhancement factors, with the peak flux enhancement ranging from ~ 1.2 to 2200 times. The variation in the resonance energies with geomagnetic latitude has good agreement with that expected from first-order equatorial cyclotron resonance with NWC signals that have propagated through the plasmasphere inside ducts.

[34] There are almost no wisp-like enhancements produced by the transmitter NPM, despite its low-latitude location and relatively high output power. The lack of any wisp enhancement for $L < 1.6$ suggests that nonducted propagation is an inefficient mechanism for scattering electrons, which explains the lower cutoff in L of the NWC-generated wisps and the lack of NPM-generated wisps. The single example of an NPM-associated wisp is consistent with transmissions from NPM coupling into a duct at $L = 1.7$, with no significant scattering from the nonducted component known to be propagating through $L = 1.2$ to 1.5 .

[35] Finally, we consider the likelihood that ducts are both sufficiently large in L and frequently occurring enough that a $\sim 95\%$ occurrence rate from $L = 1.7$ – 1.9 could be explained solely owing to ducting. Previous studies of whistler-mode signals from the transmitter NAA, received in Rothera station, Antarctica, show that ducting occurs across the L range in which we observe NWC-driven enhancements, with an occurrence rate that is consistent with the 95% NWC wisp occurrence rate reported in this paper.

[36] **Acknowledgments.** C. J. R. and M. A. C. would like to acknowledge the funding from the LAPBIAT program (contract RITA-CT-2006-025969) for supporting their time at the Sodankylä Geophysical Observatory, where they worked on this manuscript. The work of J. A. S., M. P., and J. J. B. was supported by the Centre National d'Etudes Spatiales (CNES), while C. J. R. is a Guest Investigator inside the DEMETER program. We are grateful to the NSSDC at GSFC for providing reports on radiation belt models, and the NOAA National Geophysical Data Center for the POES data.

[37] Zuyin Pu thanks Jay Albert and Reiner Friedel for their assistance in evaluating this paper.

References

- Abel, B., and R. M. Thorne (1998), Electron scattering loss in Earth's inner magnetosphere: 1. Dominant physical processes, *J. Geophys. Res.*, **103**, 2385–2396, (Correction, *J. Geophys. Res.*, **104**, 4627–4628, 1999.).
- Baker, D. N., S. G. Kanekal, X. Li, S. P. Monk, J. Goldstein, and J. L. Burch (2004), An extreme distortion of the Van Allen belt arising from the 'Halloween' solar storm in 2003, *Nature*, **432**(7019), 878–880, doi:10.1038/nature03116.
- Berthelier, J. J., et al. (2006), ICE: The electric field experiment on DEMETER, *Planet. Space Sci.*, **54**(5), 456–471, doi:10.1016/j.pss.2005.10.016.
- Carpenter, D. L., and R. R. Anderson (1992), An ISEE/whistler model of equatorial electron density in the magnetosphere, *J. Geophys. Res.*, **97**(A2), 1097–1108.
- Chang, H. C., and U. S. Inan (1983), Quasi-relativistic electron precipitation due to interactions with coherent VLF waves in the magnetosphere, *J. Geophys. Res.*, **88**, 318–328.
- Clilverd, M., and R. Horne (1996), Ground-based evidence of latitude-dependent cyclotron absorption of whistler mode signals originating from VLF transmitters, *J. Geophys. Res.*, **101**(A2), 2355–2367.
- Clilverd, M. A., A. J. Smith, and N. R. Thomson (1991), The annual variation in quiet time plasmaspheric electron-density, determined from whistler mode group delays, *Planet. Space Sci.*, **39**, 1059–1067, doi:10.1016/0032-0633(91)90113-O.
- Clilverd, M. A., N. R. Thomson, and A. J. Smith (1993), The influence of ionospheric absorption on midlatitude whistler-mode signal occurrence from VLF transmitters, *J. Atmos. Terr. Phys.*, **55**, 1469–1477, doi:10.1016/0021-9169(93)90112-C.
- Clilverd, M., B. Jenkins, and N. Thomson (2000), Plasmaspheric storm time erosion, *J. Geophys. Res.*, **105**(A6), 12,997–13,008.
- Clilverd, M. A., C. J. Rodger, R. J. Gamble, N. P. Meredith, M. Parrot, J.-J. Berthelier, and N. R. Thomson (2008), Ground-based transmitter signals observed from satellite: Ducted or nonducted?, *J. Geophys. Res.*, **113**, A04211, doi:10.1029/2007JA012602.
- Datlowe, D. (2006), Differences between transmitter precipitation peaks and storm injection peaks in low-altitude energetic electron spectra, *J. Geophys. Res.*, **111**, A12202, doi:10.1029/2006JA011957.
- Datlowe, D. W., and W. L. Imhof (1990), Cyclotron resonance precipitation of energetic electrons from the inner magnetosphere, *J. Geophys. Res.*, **95**, 6477–6491.
- Dupont, D. G. (2004), Nuclear explosions in orbit, *Sci. Am.*, **290**, 68–75.
- Ferguson, J. A., and F. P. Snyder (1990), Computer programs for assessment of long wavelength radio communications, *Tech. Doc. 1773*, Natl. Ocean Syst. Cent., San Diego, Calif.
- Helliwell, R. A. (1965), *Whistlers and Related Ionospheric Phenomena*, Stanford Univ. Press, Stanford, Calif.
- Hess, W. N. (1968), *The Radiation Belt and Magnetosphere*, Blaisdell, London.
- Inan, U. S., T. F. Bell, J. Bortnik, and J. M. Albert (2003), Controlled precipitation of radiation belt electrons, *J. Geophys. Res.*, **108**(A5), 1186, doi:10.1029/2002JA009580.
- Inan, U. S., M. Golkowski, M. K. Casey, R. C. Moore, W. Peter, P. Kulkarni, P. Kossey, E. Kennedy, S. Meth, and P. Smit (2007), Subionospheric VLF observations of transmitter-induced precipitation of inner radiation belt electrons, *Geophys. Res. Lett.*, **34**, L02106, doi:10.1029/2006GL028494.
- Kulkarni, P., U. S. Inan, T. F. Bell, and J. Bortnik (2008), Precipitation signatures of ground-based VLF transmitters, *J. Geophys. Res.*, **113**, A07214, doi:10.1029/2007JA012569.
- Li, X. L., and M. A. Temerin (2001), The electron radiation belt, *Space Sci. Rev.*, **95**(1–2), 569–580, doi:10.1023/A:1005221108016.
- Mahajan, K. K., and L. H. Brace (1969), Latitudinal observations of the thermal balance in the nighttime protonosphere, *J. Geophys. Res.*, **74**(21), 5099–5112.
- Parrot, M., J. A. Sauvaud, J. J. Berthelier, and J. P. Lebreton (2007), First in-situ observations of strong ionospheric perturbations generated by a powerful VLF ground-based transmitter, *Geophys. Res. Lett.*, **34**, L11111, doi:10.1029/2007GL029368.
- Reeves, G. D., K. L. McAdams, R. H. W. Friedel, and T. P. O'Brien (2003), Acceleration and loss of relativistic electrons during geomagnetic storms, *Geophys. Res. Lett.*, **30**(10), 1529, doi:10.1029/2002GL016513.
- Rodger, C. J., M. A. Clilverd, and R. J. McCormick (2003), Significance of lightning generated whistlers to inner radiation belt electron lifetimes, *J. Geophys. Res.*, **108**(A12), 1462, doi:10.1029/2003JA009906.
- Rodger, C. J., M. A. Clilverd, T. Ulich, P. T. Verronen, E. Turunen, and N. R. Thomson (2006), The atmospheric implications of radiation belt remediation, *Ann. Geophys.*, **24**(7), 2025–2041, SRef-ID:1432-0576/ag/2006-24-2025.0020.
- Rodger, C. J., M. A. Clilverd, N. R. Thomson, R. J. Gamble, A. Seppälä, E. Turunen, N. P. Meredith, M. Parrot, J. A. Sauvaud, and J.-J. Berthelier

- (2007a), Radiation belt electron precipitation into the atmosphere: Recovery from a geomagnetic storm, *J. Geophys. Res.*, **112**, A11307, doi:10.1029/2007JA012383.
- Rodger, C. J., C. F. Enell, E. Turunen, M. A. Clilverd, N. R. Thomson, and P. T. Verronen (2007b), Lightning-driven inner radiation belt energy deposition into the atmosphere: Implications for ionisation-levels and neutral chemistry, *Ann. Geophys.*, **25**, 1745–1757.
- Sauvaud, J. A., T. Moreau, R. Maggiolo, J.-P. Treilhou, C. Jacquey, A. Cros, J. Coutelier, J. Rouzaud, E. Penou, and M. Gangloff (2006), High-energy electron detection onboard DEMETER: The IDP spectrometer, description and first results on the inner belt, *Planet. Space Sci.*, **54**(5), 502–511, doi:10.1016/j.pss.2005.10.019.
- Sauvaud, J. A., R. Maggiolo, C. Jacquey, M. Parrot, J.-J. Berthelier, R. J. Gamble, and C. J. Rodger (2008), Radiation belt electron precipitation due to VLF transmitters: Satellite observations, *Geophys. Res. Lett.*, **35**, L09101, doi:10.1029/2008GL033194.
- Steer, I. (2002), Briefing: High-altitude nuclear explosions; Blind, deaf and dumb (online), *Janes Def. Weekly*, **23 Oct.**, 20–23.
- Teague, M., and J. Vette (1972), The inner zone electron model AE-5, *Rep. NSSDC 72-10*, Natl. Space Sci. Data Cent., Greenbelt, Md.
- Thomson, N. R. (1987), Experimental observations of very low latitude man-made whistler-mode signals, *J. Atmos. Terr. Phys.*, **49**, 309–319, doi:10.1016/0021-9169(87)90027-4.
- Thomson, N. R. (1989), Reradiation of VLF radio-waves from mountain ranges, *J. Atmos. Terr. Phys.*, **51**, 339–349, doi:10.1016/0021-9169(89)90084-6.
- U.S. Congress (2001), Space: Today and the future, in *Report of the Commission to Assess United States National Security, Space Management and Organization*, chap. 2, pp. 21–22, 11 Jan., Space Comm., Washington, D. C. (Available at <http://www.dod.mil/pubs/space20010111.html>)
- Van Allen, J. A. (1997), Energetic particles in the Earth's external magnetic field, in *Discovery of the Magnetosphere, Hist. Geophys.*, vol. 7, edited by C. S. Gillmor and J. R. Spreiter, pp. 235–251, AGU, Washington, D. C.
- Van Allen, J. A., G. H. Ludwig, E. C. Ray, and C. E. McIlwain (1958), Observation of high intensity radiation by satellites 1958 Alpha and Gamma, *Jet Propul.*, **28**, 588–592.
- Walt, M. (1994), *Introduction to Geomagnetically Trapped Radiation*, Cambridge Univ. Press, Cambridge, U.K.
- Walt, M. (1996), Source and loss processes for radiation belt particles, in *Radiation Belts: Models and Standards, Geophys. Monogr. Ser.*, vol. 97, edited by J. F. Lemaire et al., pp. 1–13, AGU, Washington, D. C.
- Winter, J., et al. (2004), A proposed large deployable space structures experiment for high power, large aperture missions in MEO, in *2004 IEEE Aerospace Conference Proceedings*, vol. 1, p. 532, doi:10.1109/AERO.2004.1367636, IEEE Press, Piscataway, N. J.
- J.-J. Berthelier, Centre d'Etudes des Environnements Terrestre et Planétaires, 4 Avenue de Neptune, F-94107 Saint Maur des Fosses, France. (jean-jacques.berthelier@cetp.ipsl.fr)
- M. A. Clilverd, Physical Sciences Division, British Antarctic Survey, NERC, High Cross, Madingley Road, Cambridge CB3 0ET, UK. (m.clilverd@bas.ac.uk)
- R. J. Gamble, R. J. McCormick, C. J. Rodger, S. L. Stewart, and N. R. Thomson, Department of Physics, University of Otago, P.O. Box 56, Dunedin 9016, New Zealand. (rgamble@physics.otago.ac.nz; rmccormick@physics.otago.ac.nz; crodger@physics.otago.ac.nz; sstewart@physics.otago.ac.nz; thomson@physics.otago.ac.nz)
- M. Parrot, Laboratoire de Physique et Chimie de l'Environnement, 3A Avenue de la Recherche Scientifique, F-45071 Orleans Cedex 2, France. (mparrot@cns-orleans.fr)
- J.-A. Sauvaud, Centre d'Etude Spatiale des Rayonnements, 9 Avenue du Colonel Roche, F-31028 Toulouse Cedex 4, France. (sauvaud@cesr.fr)